Mechanics-based modelling of the seismic out-of-plane dynamic response of unreinforced masonry gables

Ziwei Dai[1][0000-0002-0177-3262], Satyadhrik Sharma[1] Nicolò Damiani[2,3], Francesco Graziotti[2,3], Francesco Messali[1]

[1] Department of Materials, Mechanics, Management & Design, Section of Applied Mechanics, Delft University of Technology–TU Delft, Delft, the Netherlands
[2] Department of Civil Engineering and Architecture – DICAr, University of Pavia, Pavia, Italy
[3] European Centre for Training and Research in Earthquake Engineering – EUCENTRE, Pavia, Italy
z.dai-1@tudelft.nl

Abstract. Unreinforced masonry (URM) gables, common in low-rise buildings with pitched roofs, exhibit notable vulnerability under seismic excitation, as observed in regions like Groningen, Netherlands, experiencing induced seismicity. This study introduces a computationally efficient three-degree-of-freedom (3-DOF) model to accurately predict the out-of-plane (OOP) dynamic response of URM gables under seismic loading. The model integrates global rigid-body motions induced by roof flexibility and local masonry deflections. Parameter calibration for capturing the measured response from novel shake table experiments on URM gables is conducted by employing a novel two-stage strategy based on Modified Nelder-Mead (MNM) optimization approach, enabling accurate representation of elastic and nonlinear behaviours under varied roof stiffness scenarios. Validation against full-scale incremental dynamic tests demonstrates excellent agreement in predicting the onset and progression of cracking, rocking, frictional sliding, and internal masonry degradation as well as full collapse. This simplified yet robust modeling approach offers significant potential for rapid seismic vulnerability assessment of URM structures.

Keywords: Seismic analysis, Numerical modeling, Unreinforced masonry gable, Out-of-plane deformation, Structural safety.

1 Research Overview

Low-rise unreinforced masonry (URM) buildings, common across seismic-prone regions in Europe and beyond, frequently incorporate pitched roof systems supported by masonry gables. These gables are widely recognized as among the most seismically vulnerable components, particularly in their out-of-plane (OOP) direction. Despite extensive post-earthquake evidence of gable failures, experimental studies specifically focused on URM gables remain scarce. To address this gap, full-scale shake-table tests were conducted on triangular URM gables, each 6 m wide and 3 m high, constructed from solid clay bricks with friction-based timber-to-masonry connections. Designed as numerical benchmarks, these tests captured the dynamic seismic response of gables up to collapse. Fig.1a shows the dynamic test setup of a full-scale URM gable under controlled boundary conditions, with vertical loads applied via spring-loaded timber arms to simulate realistic roof effects. Seismic inputs were applied simultaneously at the base and top (via a shake table system) to investigate the influence of roof diaphragm stiffness: rigid, semi-flexible, and flexible configurations. The tests employed incremental dynamic loading with scaled tectonic and induced seismic records to capture diverse frequency and intensity responses [1]. Building on these results, this paper presents a mechanics-based numerical model developed to reproduce the observed OOP response and failure mechanisms, with the aim of enhancing predictive capability for seismic assessment of URM gables.

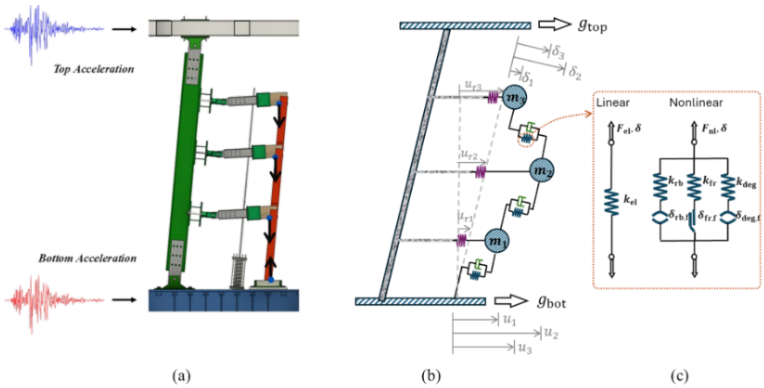

Fig. 1. Schematic of the dynamic loading setup for URM gables: (a) Experimental configuration; (b) 3DOF computational scheme; (c) Constitutive relationships.

To capture the seismic performance observed in the experiments, a 3-DOF lumped-parameter model (see Fig.1b) is proposed, vertically discretizing the URM gable into three segments with distinct mass and stiffness parameters. The displacement of each segment is expressed as $u(t) = u_{\mathrm{r}}(t) + \delta(t)$, where u_{r} denotes rigid displacement due to roof-induced rotations and translations (resulting from the experimental loading apparatus simulating roof flexibility), and δ represents local deflections attributable to masonry deformation.

In the initial elastic phase, the segment stiffness is defined as k_{el} and the roof-to-gable connection stiffness as k_{r}. Upon reaching the cracking threshold, the segment stiffness transitions into three nonlinear mechanisms (see Fig.1c):

- Rocking (k_{rb}): segment rotation at cracked interfaces;
- Friction (k_{fr}): horizontal slip at the timber-gable interface;
- Degradation (k_{deg}): internal masonry damage progression.

The total nonlinear restoring force is given by

$$F_{\mathrm{nl}} = F_{\mathrm{rb}} + F_{\mathrm{fr}} + F_{\mathrm{deg}} \tag{1}$$

Dynamic damping is represented by two coefficients: c_{r} for global motions and c_{g} for local deflections. The system equations of motion, incorporating these parameters, are solved using an explicit non-iterative Newmark scheme.

Parameter calibration utilizes a novel two-stage Modified Nelder-Mead (MNM) optimization model developed previously [5], fitting multiple roof configurations simultaneously. Parameters for masonry deformation (e.g., k_{el}) are enforced across cases, while timber connection parameters (e.g., k_{r}) vary by roof type.

A 3DOF Newmark solver computes the dynamic response, particularly the time histories of deflection and acceleration. The MNM algorithm iteratively adjusts the parameter set within realistic bounds to minimize difference between simulated and experimental curves. Elastic parameters are first calibrated using low-intensity responses, followed by nonlinear parameters capturing rocking, friction, and degradation based on moderate-to-high-intensity tests. The calibrated parameters are further validated by analytically derived results to ensure their reliability. The computational efficiency of the framework enables hundreds of iterations within minutes, ensuring rapid and reliable convergence.

2 Results

The dynamic response and hysteretic behaviour of the gable are illustrated in Fig.2 for the representative rigid roof configuration. Fig.2(a) compares the time history of the maximum deflection (δ_{max}) between experiment and simulation for the last three input intensities, showing good agreement in amplitude and phase. Fig.2(b) presents the total inertial force (F) vs. δ_{max} with the simulated response closely matching the experimental results across both pre- and post-cracking phases.

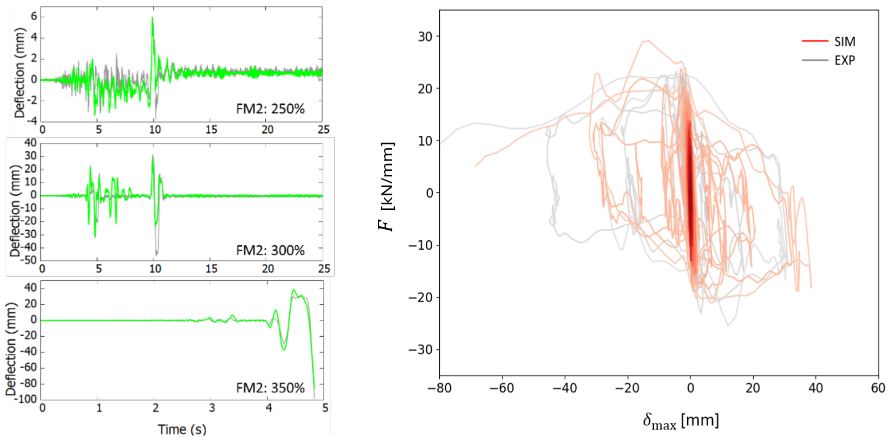

(a) Deflection-time histories (b) Force–deflection hysteretic response

Fig. 2. Comparison of experimental and numerical results.

Incremental Dynamic Analysis (IDA) curves are constructed by incrementally applying seismic inputs of increasing intensity, with the peak bottom table acceleration (PBA) plotted against the corresponding δ_{max}. At low input intensities, the structure exhibits a predominantly elastic response, as indicated by the nearly linear trend. As the intensity increases, a significant reduction in stiffness is observed, eventually leading to collapse. The dashed portion of the curve denotes extrapolated trends beyond structural collapse. The model successfully captures and closely reproduces the experimental trends across the entire loading process.

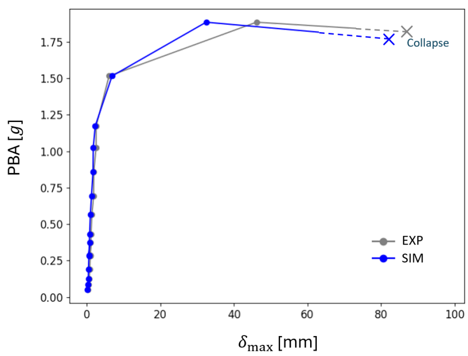

Fig. 3. Incremental Dynamic Analysis (IDA) curves: experimental vs. numerical.

The trilinear force-displacement idealizations proposed by Doherty et al. [6] and Griffith et al. [7] form the conceptual basis for representing rocking, sliding, and degradation mechanisms in URM walls. By incorporating these mechanisms into the present mechanics-based model, the simulated IDA curves naturally reflect a progressive response evolution that qualitatively aligns with the expected structural behaviour under increasing seismic intensity

3 Conclusions

The presented computational framework demonstrates significant advantages for seismic safety assessment of URM gables:

(1) Accurately predicts the influence of roof stiffness configurations on gable seismic response and failure modes.
(2) Distinguishes effectively between global roof-induced motions and local masonry deformation mechanisms, enhancing physical interpretability.
(3) Employs the efficient MNM-Newmark calibration method, offering rapid and precise fitting of both elastic and nonlinear parameters.

Future research will extend this model to accommodate analyses of URM gable walls with diverse geometries, structural configurations, and boundary conditions, thus broadening its applicability to a wider range of masonry structures and scenarios.

References

1. Sharma S, Damiani N, Bertassi M, Smerilli M, Mirra M, Lanese I, Rizzo Parisi E, O'Reilly GJ, Messali F, Graziotti F (2025) Experimental data from out-of-plane shake-table tests on unreinforced masonry gables. Earthquake Spectra (in review).
2. Tomassetti U, Correia AA, Graziotti F, Penna A (2019) Seismic vulnerability of roof systems combining URM gable walls and timber diaphragms. Earthquake Engineering & Structural Dynamics 48: 1297–1318.
3. Godio M, Beyer K (2017) Analytical model for the out-of-plane response of vertically spanning unreinforced masonry walls. Earthquake Engineering & Structural Dynamics 46: 2757–2776.
4. Sharma S, Bouwmeester H, Graziotti F, Messali F (2025) Numerical simulation of the dynamic out-of-plane two-way bending seismic behaviour of unreinforced masonry walls using equivalent SDOF systems. In: Milani G, Ghiassi B (eds) 18th International Brick and Block Masonry Conference. IB2MaC 2024. Lecture Notes in Civil Engineering, vol 613. Springer, Cham.
5. Dai Z, Zhu X, Gilabert FA (2023) A multi-material-oriented modeling framework to characterize and predict mechanical self-healing. International Journal of Mechanical Sciences 260: 108644.
6. Doherty K, Griffith MC, Lam N, Wilson J (2002) Displacement-based seismic analysis for out-of-plane bending of unreinforced masonry walls. Earthquake Engineering and Structural Dynamics 31: 833-850.
7. Griffith MC, Lam NTK, Wilson JL, Doherty K (2004) Experimental investigation of unreinforced brick masonry walls in flexure. Journal of Structural Engineering 130(3): 423–432.